



## Theory of isobaric pressure exchanger for desalination

Chiang C. Mei<sup>a,\*</sup>, Ying-Hung Liu<sup>b</sup>, Adrian W-K. Law<sup>c</sup>

<sup>a</sup>Department of Civil and Environmental Engineering, Massachusetts Institute of Technology, Cambridge, MA, USA 02139  
Tel. +1 617 253 2994; Fax: +1 617 253 6300; email: ccmei@mit.edu

<sup>b</sup>Department of Civil and Environmental Engineering, Massachusetts Institute of Technology, Cambridge, MA, USA 02139

<sup>c</sup>School of Civil and Environmental Engineering, Nanyang Technological University, Singapore

Received 12 May 2011; Accepted 11 August 2011

---

### ABSTRACT

A theory is developed to predict the time of sustained operation of a rotary pressure exchanger used for energy recovery in seawater reverse osmosis system. Based on past experiments for oscillating pipe flows, it is found that the existing plug flow velocity in the ducts is not high enough to induce turbulence in the wall boundary layer. Modeling the time series of the flow velocity in the inviscid core as a periodic series of rectangular pulses, the structure of the laminar momentum boundary layer is first derived. The mass boundary layer induced by the oscillating velocity is then solved in order to obtain the slow diffusion of the averaged brine concentration along the duct. With the result the effective longitudinal diffusivity (dispersivity) is found explicitly for arbitrary Schmidt number. The dispersivity is found to be small due to the small viscosity and mass diffusivity in the very thin boundary layers, however it is still augmented to hundreds times of the molecular diffusivity. For a range of duct and rotor dimensions and rotor frequencies, the time needed for the mixing zone to spread to the ends of the duct is predicted for large Schmidt number appropriate for salt in water. After transient mixing is over, a certain amount of salt leaks steadily into the fresh seawater reentering the membrane. However the leakage is shown to be small due to the small dispersivity.

*Keywords:* Pressure exchanger; SWRO system; Energy recovery; Boundary-layer theory; Convective diffusion; Taylor dispersion

---

### 1. Introduction

Desalination plants have been in operation for years at many coastal sites not only for producing drinking water but also for treating waste water generated from oil production fields [1]. In the technology of desalination by sea water reverse osmosis (SWRO), salt is removed by applying very high pressure up to 80 bars to force sea water against a semi-permeable membrane. Energy needed in such a process can consume as high as 70%

of the total cost [2]. As a result several types of energy recovery devices (ERD) have been designed to reclaim the high pressure remaining in the brine reject. Among these the isobaric pressure exchanger (PX) seems to be the most efficient [3,4]. The central part of the design is a rotor with several ducts of small radius distributed along a circle of large radius, as shown in Fig. 1. At any instant the right half of a duct is filled with brine reject and the left half with fresh seawater. During one half of the rotation cycle, several ducts are open to the inlet A and the outlet B. A fixed volume of brine reject enters the right end and instantly passes the high pressure to the fresh

---

\*Corresponding author.

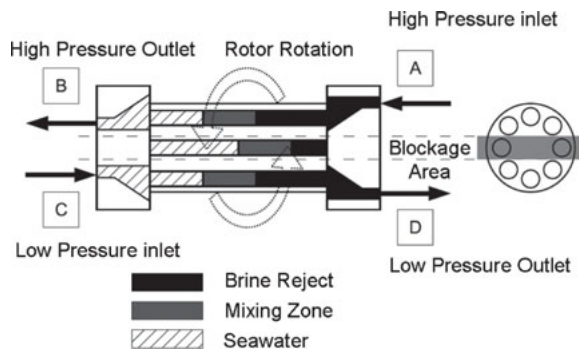


Fig. 1. SWRO system and isobaric pressure exchanger. From [3].

sea water. The same volume of seawater is pushed out of B, and joins the flow in the outgoing pipe towards the membrane. This is followed by a short period of blockage during which there is no flow in the duct. In the next half cycle after passing a blocked sector, the same duct is open to the feeder pipe at the left end and to the brine outfall at low pressure at the right end. Fresh sea water enters C and discharges the brine reject at D. After passing another blocked sector the same duct is open at the inlet A again to receive new brine reject for the second cycle, etc.

Because there are many ducts in the same rotor, the brine reject and the seawater flow steadily through the system but at opposite ends of each duct, recycling the high pressure continuously.

At the moment of switch-on there is a pulsating interface near the middle of the duct separating the fresh sea water from the brine reject. Diffusion will change the interface into a broad zone of mixing. In existing systems the typical rotor dimensions are: duct length = 1 m, rotor radius = 0.2 m and duct radius = 0.01 m [3]. The rotor speed lies between 500 to 2000 rpm. An array of 40 rotor units can be installed at a plant. Such units are attractive not only for on-land installations but also on desalination vessels for serving offshore sites.

An isobaric pressure exchanger should be designed to avoid as much as possible adding more salt to the flow reentering the membrane from the high-pressure outlet B of the system. While the design can be guided by laboratory tests, mathematical models can be useful as economical alternatives. Based on the assumption of full turbulence in the ducts, a numerical analysis based on  $k$ - $\epsilon$  model has been reported by [5]. This assumption is however at variance with laboratory studies for oscillatory flows in pipes of comparable radius. Motivated by other reasons, Hino and Ohmi et al. have shown for a pipe flow under a sinusoidal pressure gradient that transition to turbulence takes place when the Reynolds number  $Re_\delta = U \delta / \nu$  can be higher than 760, where  $U$  is

the characteristic velocity,  $\nu$  the fluid kinematic viscosity and  $\delta = \sqrt{2\nu/\omega}$  is the Stokes boundary layer thickness and  $\omega$  the oscillation frequency [6,7]. By numerical simulation the critical Reynolds number is found by Ahn & Ibrahim to be

$$Re_\delta = 336.75 \left( \frac{a_0}{\delta} \right)^{1/7} \quad (1)$$

which shows a weak dependence on the ratio  $a_0/\delta$ , where  $a_0$  is the pipe radius [8]. Motivated by flows in blood vessels, Akahaven et al. have carried out extensive laboratory and numerical studies in simple-harmonic pipe flows, and concluded that transition to turbulence occurs roughly when  $Re_\delta = 500$ – $550$  [9,10]. Similar experiments by Eckman & Grotberg also found that transition to turbulence in a tube of diameter 1.25 inches occurs during the decelerating phase when  $500 < Re_\delta < 854$  for  $9 < a_0/\sqrt{\nu/\omega} < 33$  [11].

In the duct of a pressure exchanger, the plug flow is not simple harmonic but a periodic series of intermittent pulses of alternating signs. Let  $T_0$  be the duration of blockage per half rotation and  $T = 2\pi/\omega$  the rotation period. Their ratio depends on the inlet design. If only one duct is blocked during each half cycle, the ratio can be estimated by  $T_0/T = O(a_0/\pi r_0)$  where  $r_0$  is the radial distance from the duct center to the rotor axis. Using a generous estimate of the duct velocity 5 m/s, we get  $Re_\delta \sim 700$ . Hence duct flow is likely laminar under many operating conditions. A theory of convective diffusion in laminar oscillatory flow is called for.

Following the pioneering work of G.I. Taylor [12] on convective diffusion (i.e., dispersion) in steady channel flows, theories for sinusoidal laminar pipe flows have been advanced in [12–15]. In this article we extend their theories to intermittent flows in a duct with a view to predict the longitudinal dispersivity, i.e., the effective diffusivity, of the averaged concentration. The duration of transient diffusion for the mixing zone to spread across the full length of the duct will be first predicted for a range of duct and rotor dimensions, and rotor speed. To assess the efficiency of the pressure exchanger, the amount of salt transfer during the final steady state will also be calculated. Details of transient evolution of the averaged concentration as well as its quasi-periodic fluctuation will be examined.

## 2. Velocity in the duct

Because the drum is forced to rotate like a hydraulic turbine by high-pressure inflow through specially shaped inlets, detailed prediction of the velocity near the duct ends is a complex task of numerical simulation

depending on the inlet/outlet geometry. It is only known that the oscillating flow velocity is roughly proportional to the rotation frequency so that the fluid plug is kept away from the ends of the duct [3]. Because the duct radius is typically much smaller than the duct length, we shall ignore the end effects and assume the velocity to be uniform along the entire length, and its maximum amplitude is known. For generality  $T_0/T$  is assumed to range from moderate to very small values. Although the radial profile of the longitudinal velocity  $u'(r', t')$  can be found exactly in terms of Bessel functions by extending Womersley from simple-harmonic to multi-harmonic flows, it is sufficient for present purposes to employ the boundary layer approximation because of the small viscosity [16].

Using primes to denote physical variables, we let the velocity profile be the sum of the inviscid core velocity  $W'(t')$  (plug-flow velocity) and the correction in the viscous boundary-layer  $V' = (r', t')$

$$u'(r', t') = W'(t') + V'(r', t') \tag{2}$$

2.1. Inviscid core

The plug-flow velocity  $W'(t')$  is a periodic series of intermittent pulses of alternating signs. Let all dimensionless variables be without primes. Defining the dimensionless time by  $t = \omega t'$ , we expand the series of pulses as an odd Fourier series in  $-\pi < t < \pi$ ,

$$\begin{aligned} W'(t') = \mathbf{U}W(t) &= \mathbf{U} \sum_{n=-\infty}^{\infty} W_n e^{-int} \\ &= 2\mathbf{U} \sum_{n=1}^{\infty} W_n \sin(nt) \end{aligned} \tag{3}$$

then

$$W_n = \frac{\int_0^\pi W(t) \sin(nt) dt}{2 \int_0^\pi \sin^2(nt) dt} = \frac{1}{\pi} \int_0^\pi W(t) \sin(nt) dt \tag{4}$$

The crudest model of the plug-flow velocity is a series of rectangular pulses

$$W = \begin{cases} 0, & 0 \leq t \leq c; \\ 1, & c \leq t \leq \pi - c; \\ 0, & \pi - c \leq t \leq \pi; \end{cases} \tag{5}$$

where  $2c/\pi = 2T_0/T$  is the fraction of blockage time in a half-period. It is easy to find

$$\begin{aligned} W_n &= \frac{1}{\pi} \int_c^{\pi-c} \sin(nt) dt = \frac{2}{n\pi} \cos(nc), \\ n &= \text{odd}; W_n = 0, n = \text{even} \end{aligned} \tag{6}$$

which converges slowly. Because it takes finite time for a circular duct to be fully open to the inlet flow, a slightly more realistic model is a series of rectangles with rounded corners

$$W(t) = \begin{cases} 0, & 0 \leq t \leq c; \\ \frac{1}{2} \left[ 1 + \cos \left( \frac{\pi(t-(c+b))}{b} \right) \right], & c \leq t \leq c+b; \\ 1, & c+b \leq t \leq \pi-(c+b); \\ \frac{1}{2} \left[ 1 - \cos \left( \frac{\pi(t-(\pi-c))}{b} \right) \right], & \pi-(c+b) \leq t \leq \pi-c; \\ 0, & \pi-c \leq t \leq \pi \end{cases} \tag{7}$$

More accurate computation of  $W(t)$  accounting the duct/rotor geometry is possible but it will only affect the details of  $W_n$  and not the essential physics. In this article the rounded rectangles will be used with the special choice<sup>1</sup> of  $c = 2b$  for simplicity. The lengthy expression of  $W_n$  is given in Appendix A. A sample time series of  $W(t)$  is shown in Fig. 2.

2.2. Boundary layer correction

The boundary-layer correction is governed by

$$\frac{\partial V'}{\partial t'} = \frac{\nu}{r'} \frac{\partial}{\partial r'} \left( r' \frac{\partial V'}{\partial r'} \right) \tag{8}$$

subjected to the boundary conditions:

$$V' = -W', r' = a_0; \text{ and } \frac{\partial V'}{\partial r'} = 0, r' = 0 \tag{9}$$

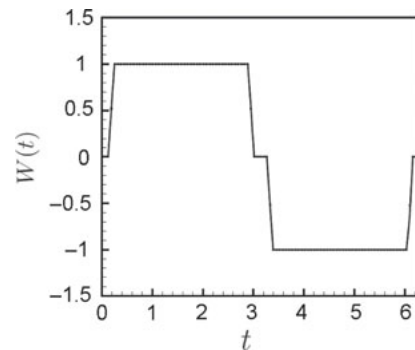


Fig. 2. Model of velocity pulses in the inviscid core as smoothed rectangles with  $c = 2b = 0.15$ .

<sup>1</sup>It has been found that the numerical results computed from the two models are quite close.

With the normalization:

$$(u', W', V') = \mathcal{U}(u, W, V), t' = \frac{t}{\omega}, r' = a_0 r \quad (10)$$

Eq. (8) becomes

$$\frac{\partial V}{\partial t} = \frac{\varepsilon^2}{r} \frac{\partial}{\partial r} \left( r \frac{\partial V}{\partial r} \right) \quad (11)$$

The typical values of the scales are  $\mathcal{U} = 1$  m/s,  $\omega = 100$  rad/s,  $a_0 = 1.5$  cm,  $\nu = 10^{-2}$  cm<sup>2</sup>/s, hence the inverse of the Stokes-Womersley number defined by

$$\varepsilon = \frac{1}{a_0} \sqrt{\frac{\nu}{\omega}} \ll 1, \quad (12)$$

is very small. The boundary conditions are

$$V(1, t) = -W, \text{ and } \frac{\partial V(0, t)}{\partial r} = 0 \quad (13)$$

Let

$$V = \sum_{n=-\infty}^{\infty} V_n e^{-int} \quad (14)$$

then

$$-iV_n = \frac{\varepsilon^2}{n} \frac{1}{r} \frac{\partial}{\partial r} \left( r \frac{\partial V_n}{\partial r} \right) = \frac{\varepsilon^2}{n} \left( \frac{\partial^2 V_n}{\partial r^2} + \frac{1}{r} \frac{\partial V_n}{\partial r} \right) \quad (15)$$

with the boundary conditions:

$$V_n(1) = -W_n, \quad \frac{\partial V_n(0)}{\partial r} = 0 \quad (16)$$

Similar to the simple harmonic case treated by Watson [15], we introduce the boundary layer coordinate (see Fig. 3),

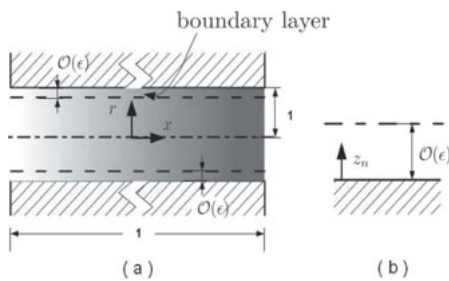


Fig. 3. Geometry in dimensionless coordinates. (a) The duct. (b) The boundary layer magnified.

$$z_n = \frac{1-r}{\varepsilon/\sqrt{n}} \quad (17)$$

then,

$$-iV_n = \frac{\partial^2 V_n}{\partial z_n^2} - \frac{1}{\sqrt{n}} \frac{\partial V_n}{\partial z_n} = \frac{\partial^2 V_n}{\partial z_n^2} + O\left(\frac{\varepsilon}{\sqrt{n}}\right) \quad (18)$$

The leading-order solution is

$$V_n^{(0)} = -W_n e^{-\sqrt{-i}z_n} \quad (19)$$

which diminishes to zero exponentially outside the boundary layer ( $z_n \gg 1$ ).

In summary the dimensionless velocity everywhere is

$$u(r, t) = \sum_{n=-\infty}^{\infty} U_n e^{-int} \quad (20)$$

where

$$U_n = W_n \left( 1 - e^{-\sqrt{-i}z_n} + O\left(\frac{\varepsilon}{\sqrt{n}}\right) \right) \quad (21)$$

to the leading order. The amplitudes of  $U_n$  and  $u$  depend on two parameters,  $c$  and  $\varepsilon$ .

### 3. Effective equation for salt diffusion

We consider diffusion in a duct of finite length  $-L/2 < x' < L/2$ , and begin with the exact equation for salt concentration  $C'$ :

$$\frac{\partial C'}{\partial t'} + u'(r', t') \frac{\partial C'}{\partial x'} = D \left( \frac{\partial^2 C'}{\partial x'^2} + \frac{1}{r'} \frac{\partial}{\partial r'} \left( r' \frac{\partial C'}{\partial r'} \right) \right) \quad (22)$$

Let

$$C' = C'_0(x', t') + C'_1(x', r', t') \quad (23)$$

where

$$C'_0(x', t') \equiv \overline{C'} \quad (24)$$

is the time and area average defined by

$$\langle f \rangle = \frac{2\pi}{\pi a^2} \int_0^a r' f(r', t') dr', \quad \bar{f} = \frac{\omega}{2\pi} \int_0^{2\pi/\omega} f(r', t') dt' \quad (25)$$

Thus

$$\overline{\langle C'_1 \rangle} = 0 \quad (26)$$

and  $C'(x', r', t')$  is the deviation from the average. We expect that

$$C'_1 \ll C'_0, \quad \frac{\partial}{\partial x'} \ll \frac{\partial}{\partial r'} \quad (27)$$

and that the time scale of  $C'_0$  is much longer than  $O(2\pi/\omega)$ .

Substituting Eq. (23) in Eq. (22) and taking the area and time average, we get

$$\frac{\partial C'}{\partial t'} + \left\langle u' \frac{\partial C'}{\partial x'} \right\rangle = D \frac{\partial^2 C'}{\partial x'^2} \quad (28)$$

since  $\overline{u'} = 0$ . The difference of Eq. (22) and Eq. (28) is

$$\begin{aligned} \frac{\partial C'_1}{\partial t'} + u' \frac{\partial C'_0}{\partial x'} + u' \frac{\partial C'_1}{\partial x'} - \left\langle u' \frac{\partial C'_1}{\partial x'} \right\rangle \\ = D \frac{\partial^2 C'_1}{\partial x'^2} + \frac{D}{r'} \frac{\partial}{\partial r'} \left( r' \frac{\partial C'_1}{\partial r'} \right) \end{aligned} \quad (29)$$

Because of Eq. (27), we have, at the leading order

$$\frac{\partial C'_1}{\partial t'} + u' \frac{\partial C'_0}{\partial x'} = \frac{D}{r'} \frac{\partial}{\partial r'} \left( r' \frac{\partial C'_1}{\partial r'} \right) \quad (30)$$

From this result we infer that

$$C'_1 = O\left(\frac{\mathcal{U}}{\omega L}\right) C'_0 \quad (31)$$

Using for estimates  $\mathcal{U} = 1$  m/s,  $\omega = 100$  rad/s,  $l = 1$  m, it is evident that  $\mathcal{U}/\omega L \ll 1$ , hence  $C'_1 \ll C'_0$ , as expected.

Now assume

$$C'_1 = B(r', t') \frac{\partial C'_0}{\partial x'} \quad (32)$$

then  $B'$  is governed by

$$\frac{\partial B'}{\partial t'} + u' = \frac{D}{r'} \frac{\partial}{\partial r'} \left( r' \frac{\partial B'}{\partial r'} \right) \quad (33)$$

with the boundary conditions

$$\frac{\partial B'}{\partial r'} = 0, \quad r' = 0, a_0 \quad (34)$$

Once  $B'$  is solved, the solution can be substituted in Eq. (28) to get the effective diffusion equation for the area- and period-averaged concentration:

$$\frac{\partial C'_0}{\partial t'} + \langle \overline{u'B'} \rangle \frac{\partial^2 C'_0}{\partial x'^2} = D \frac{\partial^2 C'_0}{\partial x'^2}, \quad (35)$$

namely,

$$\frac{\partial C'_0}{\partial t'} = (D + D') \frac{\partial^2 C'_0}{\partial x'^2}, \quad (36)$$

where

$$D' = -\langle \overline{u'B'} \rangle \quad (37)$$

is the dispersion coefficient (or dispersivity).

Let us introduce the additional dimensionless variables

$$C'_0 = C_s C_0, \quad C'_1 = \frac{\mathcal{U}}{\omega L} C_s C_1, \quad B' = \frac{\mathcal{U}}{\omega} B, \quad x' = Lx, \quad (38)$$

where  $C_s$  is the concentration of the seawater. The scale of  $B'$  is inferred from Eq. (31) and Eq. (32). In normalized variables,  $B$  is governed by

$$\frac{\partial B}{\partial t} + u = \frac{\varepsilon^2}{S_c} \frac{1}{r} \frac{\partial}{\partial r} \left( r \frac{\partial B}{\partial r} \right), \quad 0 < r < 1 \quad (39)$$

where

$$S_c = \frac{\nu}{D} \quad (40)$$

is the Schmidt number.  $B$  must also satisfy the boundary conditions

$$\frac{\partial B}{\partial r} = 0, \quad r = 0, 1 \quad (41)$$

Finally the dimensional and dimensionless dispersion coefficients are related by

$$D' = \frac{\mathcal{U}^2}{\omega} D, \quad D = -\langle \overline{u'B'} \rangle \quad (42)$$

#### 4. Boundary layer solution for $B$

In view of Eq. (20) and Eq. (21), we assume

$$B = \sum_{m=-\infty}^{\infty} B_m e^{-imt}, \quad (43)$$

Then  $B_m$  is governed by

$$-imB_m + U_m = \frac{\varepsilon^2}{S_c} \frac{1}{r} \frac{\partial}{\partial r} \left( r \frac{\partial B_m}{\partial r} \right) \quad (44)$$

and the boundary conditions:

$$\frac{\partial B_m}{\partial r} = 0, \quad r = 0, 1. \quad (45)$$

Note that  $B_0 = 0$  since  $U_0 = 0$ .

Using the boundary-layer coordinate  $z_m$  defined for the velocity profile, the leading-order approximation of Eq. (44) is governed by

$$-imS_c B_m + S_c U_m = m \frac{\partial^2 B_m}{\partial z_m^2}, \quad 0 < z_m < \frac{\sqrt{m}}{\varepsilon} \gg 1 \quad (46)$$

and

$$\frac{\partial B_m}{\partial z_m} = 0, \quad z_m = 0, \infty \quad (47)$$

Let  $B_m$  be the sum of homogeneous and inhomogeneous parts

$$B_m = B_m^I + B_m^H \quad (48)$$

It is easy to find by boundary layer approximation

$$B_m^I = -i \frac{W_m}{m} \left( 1 + \frac{S_c}{1 - S_c} e^{-\sqrt{-iz_m}} \right) \quad (49)$$

and

$$B_m^H = i \frac{W_m}{m} \frac{\sqrt{S_c}}{1 - S_c} e^{-\sqrt{-iS_c} z_m} \quad (50)$$

Hence

$$B_m = -i \frac{W_m}{m} \left( 1 + \frac{S_c}{1 - S_c} e^{-\sqrt{-iz_m}} \right) + i \frac{W_m}{m} \frac{\sqrt{S_c}}{1 - S_c} e^{-\sqrt{-iS_c} z_m} \quad (51)$$

The solution here is a straightforward extension of of Watson for the simple harmonic case [15]. Note that both  $U_m$  and  $B_m$  are essentially constant across the duct except in the velocity and mass boundary layers. For salt in water,  $D = 1.62 \times 10^{-9} \text{ m}^2/\text{s}$ , and  $\nu = 10^{-6} \text{ m}^2/\text{s}$ , hence the Schmidt number  $S_c = 617.28$  is very large. The concentration boundary layer is much thinner than the velocity boundary layer. Eq. (51) can be well approximated simply by

$$B_m(r) = -i \frac{W_m}{m} \left( 1 - e^{-\sqrt{-iz_m}} + \frac{1}{\sqrt{S_c}} e^{-\sqrt{-iS_c} z_m} + O(S_c^{-1}) \right), \quad S_c \gg 1 \quad (52)$$

#### 5. The dimensionless dispersion coefficient

The dimensionless dispersion coefficient is

$$\begin{aligned} D &= -\langle u'B' \rangle = -\left\langle \sum_{n=-\infty}^{\infty} U_n e^{-int} \sum_{m=-\infty}^{\infty} B_m e^{-imt} \right\rangle \\ &= -2 \operatorname{Re} \sum_{n=1}^{\infty} \langle U_n B_n^* \rangle \end{aligned} \quad (53)$$

where asterisks denote the complex conjugates.

Let us derive the dispersivity for arbitrary  $S_c$ . Transforming to boundary-layer coordinates  $z_n = (1-r)/(\varepsilon\sqrt{n})$  and taking the area average, we get after some algebra,

$$\begin{aligned} \langle U_n B_n^* \rangle &= \int_0^1 2r dr W_n \left( 1 - e^{-\sqrt{-iz_n}} \right) \left( \frac{iW_n}{n} \right) \\ &\quad \times \left( 1 + \frac{S_c}{1 - S_c} e^{-\sqrt{-iz_n}} - \frac{\sqrt{S_c}}{1 - S_c} e^{-\sqrt{-iS_c} z_n} \right) \\ &= \frac{2\varepsilon}{\sqrt{n}} \left( \frac{iW_n^2}{n} \right) \left[ \frac{\sqrt{n}}{2\varepsilon} - \sqrt{2} - \frac{S_c}{\sqrt{2}(1 - S_c)} \right. \\ &\quad \left. + \frac{\sqrt{S_c}}{\sqrt{2}(1 - S_c^2)} \left( 1 + \sqrt{S_c} - i(-1 + \sqrt{S_c}) \right) \right] \end{aligned} \quad (54)$$

Hence

$$\begin{aligned} -2 \operatorname{Re} \sum_{n=1}^{\infty} \langle U_n B_n^* \rangle &= \frac{4}{\sqrt{2}} \frac{\varepsilon}{\sqrt{n}} \left( \frac{W_n^2}{n} \right) \frac{\sqrt{S_c}}{1 - S_c^2} (1 - \sqrt{S_c}) \\ &= \frac{4}{\sqrt{2}} \frac{\varepsilon}{\sqrt{n}} \left( \frac{W_n^2}{n} \right) \frac{\sqrt{S_c}}{(1 + \sqrt{S_c})(1 + S_c)} \end{aligned} \quad (55)$$

which is positive. This positiveness can be proven from Eq. (44) and Eq. (45) without resorting to their explicit solution. Finally

$$D = \varepsilon \sum_{n=1}^{\infty} \frac{4}{\sqrt{2n}} \frac{W_n^2}{n} \frac{\sqrt{S_c}}{(1 + \sqrt{S_c})(1 + S_c)} \quad (56)$$

The small factor  $O(\varepsilon)$  arises from the small thickness of the boundary layer, where dispersion is produced by shear. In general  $D$  depends on  $\varepsilon$ ,  $c$  and  $S_c$ . For salt in water  $S_c = 617.28 \gg 1$ .  $D$  can be approximated by the simple formula

$$D = \frac{\varepsilon}{S_c} \sum_{n=1}^{\infty} \frac{4}{\sqrt{2n}} \frac{W_n^2}{n} \quad (57)$$

This limiting result, which can also be derived quickly by using the approximate formula Eq. (52), will now be employed to predict the performance of the isobaric pressure exchanger.

### 6. Dispersivity and the performance of the pressure exchanger

The following values of duct and rotor radii are typical in existing designs:  $0.015 < a_0 < 0.05$  m and  $0.20$  m  $< r_0 < 0.60$  m [3]. In order to have sufficiently high flow rate only a few of the many ducts should be blocked, hence the blockage parameter  $c$  is likely a small number. Fig. 4 shows the variation of the dimensionless dispersivity  $D/\varepsilon$  for different blockage parameters and Schmidt numbers. Expectedly  $D/\varepsilon$  decreases with decreasing mass diffusivity, hence with increasing  $S_c$ . It is interesting that for salt and water  $S_c = 617.28$ ,  $D/\varepsilon$  changes very little with the blockage parameter.

Since the rotor is driven as a turbine by the high pressure inflow, the plug flow velocity  $U$  is nearly proportional to the frequency  $\omega$  so that the maximum amplitude

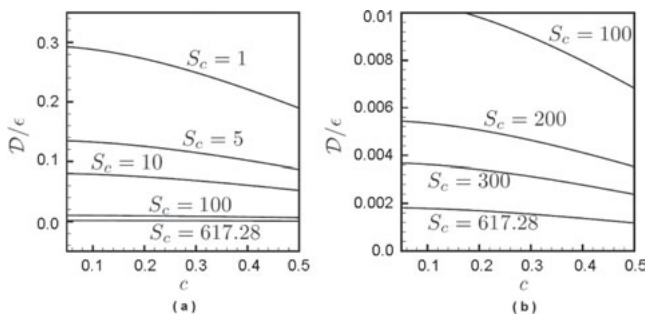


Fig. 4. The ratio  $D/\varepsilon$  for different blockage ratios  $c$  and Schmidt numbers. (a): Overview for  $1 < S_c < 617.28$ , (b): Enlarged view for  $100 < S_c < 617.28$ . For salt in water  $S_c = 617.28$ .

of the interface displacement is nearly a constant equal to a few duct radii [3]. To have some quantitative idea of the dispersivity in physical dimensions, we consider only salt and water mixture and take a typical pressure exchanger with duct radius  $a_0 = 0.015$  m, and rotor radius  $r_0 = 0.20$  m. Let the rotating frequency be  $\omega = 150$  rad/s and plug flow speed be  $U = 3$  m, implying that the order of magnitude of the interface displacement is  $X = \frac{U}{\omega}$  cm. The physical dispersivity is calculated to be  $5.72 \times 10^{-7}$  m<sup>2</sup>/s. Compared with the molecular diffusivity of salt in water  $D = 1.62 \times 10^{-9}$  m<sup>2</sup>/s, the physical dispersivity  $D'$  is greater by a factor of  $O(300)$ . Note that the boundary layer thickness is  $\delta = 1.15 \times 10^{-4}$  m and the Reynolds number is  $Re_\delta = 346.4$ , well below the threshold of turbulence.

#### 6.1. Duration of transient dispersion

Now for a duct of length  $L$ , the time scale for a sharp concentration discontinuity to spread from the middle to the ends is roughly,

$$T_L = \frac{(L/2)^2}{D + D'} \approx \frac{L^2}{4D'} \quad (58)$$

Beyond this time diffusive transfer of salt will take place steadily from the brine reject into the feeder pipe. As an example, let the length be  $L=1$  m, the time for continuous operation is roughly  $T_L = 121$  h or 5 d. Multiplying the duct length by  $N$  increases  $T_L$  by  $N^2$  times. Longer ducts are clearly better for delaying the steady transfer.

Note that from our theory,

$$D' = \frac{U^2 \varepsilon}{\omega} \frac{D}{\varepsilon} = \frac{X^2 \omega^2}{\omega} \frac{1}{a_0} \frac{D}{\varepsilon} = \frac{X^2}{a_0} \sqrt{\frac{\omega}{\nu}} \frac{D}{\varepsilon}, \quad X \equiv \frac{U}{\omega} \quad (59)$$

and  $D/\varepsilon$  depends only on  $c$  for fixed  $S_c$ . Increasing the rotor frequency by a factor  $N$  will increase  $D'$  by a factor of  $\sqrt{N}$ . The operating time  $T_L$  is reduced by a factor of  $1/\sqrt{N}$ . On the other hand  $D'$  is inversely proportional to the duct radius  $a_0$ , hence can be made smaller by using a larger duct. This likely calls for a larger rotor in order to have a fixed number of ducts per rotor. The interface displacement  $X$  should be kept as small as  $O(a_0)$  in order to keep the mixing zone close to the middle for a long time. Sample predictions on the effects of rotor frequency and duct radius are shown in Tables 1 and 2 respectively.

#### 6.2. Steady leakage

Beyond the stage of transient mixing, a steady gradient of the salt concentration is reached so that there is

Table 1

Effect of rotor frequency  $\epsilon$  for fixed  $X = 0.02$  m,  $L = 1$  m,  $a_0 = 0.015$  m and  $r_0 = 0.2$  m

$U$ (m/s)	$\omega$ (rad/s)	$\delta$ (m)	$Re_\delta$	$\mathcal{D}'$ (m <sup>2</sup> /s)	$T_L$ (h)
1.0	50	$2.00 \times 10^{-4}$	200.0	$3.30 \times 10^{-7}$	209.4
2.0	150	$1.15 \times 10^{-4}$	346.4	$5.72 \times 10^{-7}$	121.2
3.0	200	$8.94 \times 10^{-5}$	447.2	$7.37 \times 10^{-7}$	93.9

Table 2

Effect of duct radius  $a_0$  for fixed  $c = 2a_0/r_0 = 0.15$ ,  $L = 1$  m,  $U = 3$  m/s and  $\omega = 150$  rad/s.  $\delta = 1.15 \times 10^{-4}$  m and  $Re_\delta = 346.4$ 

$a_0$ (m)	$\mathcal{D}'$ (m <sup>2</sup> /s)	$T_L$ (h)
0.015	$5.72 \times 10^{-7}$	121.2
0.03	$2.58 \times 10^{-7}$	272.3
0.05	$1.16 \times 10^{-7}$	592.9

a constant leakage of salt into the feeder pipe of fresh seawater due to dispersion,

$$F_{\text{disp}} = \mathcal{D}' \frac{C_b - C_s}{L} A \quad (60)$$

where  $C_b$  is the salt concentration in the reject from the membrane,  $C_s$  the salt concentration in the fresh seawater, and  $A = \pi a_0^2$  is the cross-sectional area of the duct. Ignoring the thin boundary layer, salt flux in the brine reject from the membrane is

$$F_{\text{rej}} = AC_b \frac{\omega}{\pi} \int_0^{\pi/\omega} W'(t') dt' = AC_b \frac{U}{\pi} \int_0^\pi W(t) dt \quad (61)$$

The fraction of leakage is

$$\frac{F_{\text{disp}}}{F_{\text{rej}}} = \frac{\mathcal{D}' (1 - C_s/C_b)}{UL \frac{1}{\pi} \int_0^\pi W(t) dt} \quad (62)$$

Using Eq. (5), we have the crude estimate

$$\frac{1}{\pi} \int_0^\pi W(t) dt = \frac{\pi - 2c}{\pi} = O(1) \quad (63)$$

In practice,  $C_s/C_b = 0.6$ ,  $U = O(1)$  m/s,  $L = O(1)$  m, and  $\mathcal{D}' = O(10^{-7})$  m<sup>2</sup>/s is small, the fraction of leakage is of the order

$$O\left(\frac{\mathcal{D}'}{uL}\right) \ll 1 \quad (64)$$

confirming the high efficiency claimed by the designers [3].

## 7. Transient evolution of salt concentration in a duct

For detailed checking of the present theory by laboratory experiments, it is useful to know the slow spreading of the mixing zone from the initial discontinuity in the middle of the duct. Let us define the dimensionless time  $\tau$  by

$$\tau = \frac{D + \mathcal{D}'}{L^2} t' \approx \frac{t'}{4T_L} \quad (65)$$

So that the dimensionless averaged salt concentration  $C_0$  satisfies

$$\frac{\partial C_0}{\partial \tau} = \frac{\partial^2 C_0}{\partial x^2}, \quad -\frac{1}{2} < x < \frac{1}{2}; \quad (66)$$

Consider the initial conditions

$$C_0(x, 0) = \begin{cases} 1, & -\frac{1}{2} < x < 0, \\ 1 + \Delta C, & 0 < x < \frac{1}{2} \end{cases} \quad (67)$$

and the boundary conditions

$$C_0'(-1/2, \tau) = C_0'(1/2, \tau) = 0 \quad (68)$$

where  $\Delta C$  is the percentage concentration difference between the brine reject and the fresh seawater. Clearly the final steady state at  $\tau \sim \infty$  is given by

$$C_0(x, \infty) = 1 + \Delta C \left( x + \frac{1}{2} \right), \quad -\frac{1}{2} < x < \frac{1}{2} \quad (69)$$

The transient state  $C'(x, \tau)$  defined by

$$C'(x, \tau) = C_0(x, \tau) - 1 - \Delta C \left( x + \frac{1}{2} \right), \quad (70)$$

satisfies Eq. (66), the initial condition

$$C_0'(x, 0) = \begin{cases} -\Delta C \left( x + \frac{1}{2} \right), & -\frac{1}{2} < x < 0, \\ -\Delta C \left( x - \frac{1}{2} \right), & 0 < x < \frac{1}{2} \end{cases} \quad (71)$$

and the boundary conditions

$$C'_0(-1/2, \tau) = C'_0(1/2, t) = 0 \tag{72}$$

By expanding  $C'_0(x, 0)$  as a Fourier series it is easy to solve for  $C'_0$  and get finally

$$C_0 = 1 + \frac{\Delta C}{2} (2x + 1) + \sum_{m=1}^{\infty} \frac{\Delta C}{m\pi} \exp\left\{\left[-(2m\pi)^2\right]\tau\right\} \sin(2m\pi x) \tag{73}$$

This series converges quickly for  $\tau > 0$ .

A sample space/time evolution of  $C'_0/C_s$  is plotted in Fig. 5 in physical variables for the typical sea-water concentration of  $C_0 = 40,750$  mg/l and brine reject concentration of 73,110 mg/l. After about 200 h, steady leakage of salt enters the feeder pipe and returns to the membrane section.

In dimensionless form, the concentration fluctuation from the mean can be obtained from

$$C_1(x, t) = B \frac{\partial C_0}{\partial x} \tag{74}$$

(cf. Eq. (32)). The dimensionless concentration fluctuation is

$$\tilde{C} = \frac{C'_1}{C_s} = \frac{U}{\omega L} C_1 = \frac{U}{\omega L} B \frac{\partial C_0}{\partial x} \tag{75}$$

For salt in water, the Schmidt number is so large that the mass boundary layer is extremely thin and  $B_m$  is essentially constant across the duct, as seen in Eq. (52). Thus,

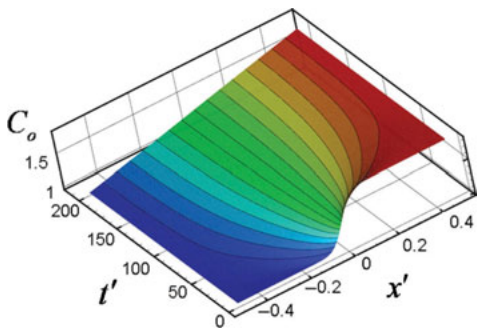


Fig. 5. Evolution of the averaged concentration  $C_0$  in physical variables  $x'$  (m) and  $t'$  (h), in a duct of  $L=1$  m,  $a_0=0.015$  m,  $r_0=0.2$  m. The rotor frequency is  $\omega=150$  rad/s and the maximum plug flow velocity is  $U=1.5$  m/s.  $D'=1.43 \times 10^{-7}$  m<sup>2</sup>/s. The blockage time fraction is assumed to be  $c=0.15$ .

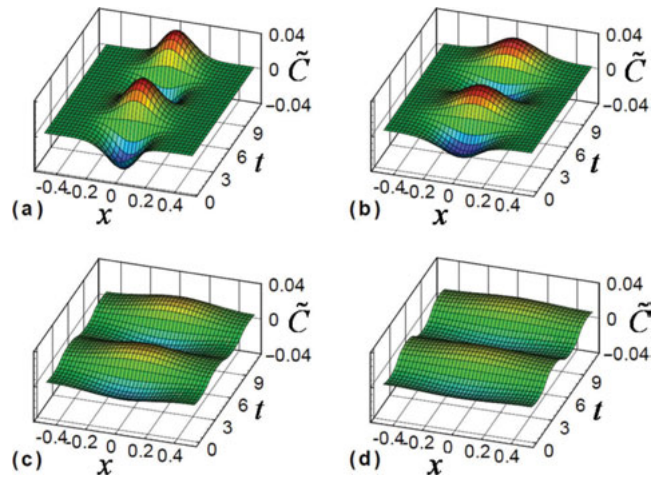


Fig. 6. Evolution of concentration fluctuation in  $\tilde{C} = C'_1/C_s$  in dimensionless variables at (a)  $\tau=0.005$  ( $t'=9.6$  h); (b)  $\tau=0.01$  ( $t'=19.2$  h); (c)  $\tau=0.03$  ( $t'=57.7$  h); (d)  $\tau=0.05$  ( $t'=96.1$  h). For a rotor with  $L=1$  m,  $a_0=0.015$  m,  $r_0=0.2$  m,  $\omega=150$  rad/s and  $U=1.5$  m/s. The blockage time fraction is assumed to be  $c=0.15$ .

$$C_1(x, t, \tau) = -\frac{\partial C_0}{\partial x} \sum_{m=-\infty}^{\infty} \frac{iW_m}{m} e^{-imt} \tag{76}$$

Recall that  $C_0(x, t)$  varies in time slowly through  $\tau$ . In Fig. 6 we show some sample results of transient fluctuations for two oscillation periods around four dimensionless times at  $\tau=0.005, 0.01, 0.03$  and  $\tau=0.05$ . For the pressure exchanger with  $L=1$  m,  $a_0=0.015$  m,  $r_0=0.2$  m,  $\omega=150$  rad/s and  $U=1.5$  m/s, we have  $U/\omega L=0.01$ . The corresponding physical times are  $t'=9.6, 19.2, 57.7$  and  $96.1$  h respectively. After such a long time the mean gradient  $\partial C'_0/\partial x'$  approaches constant along the duct. The concentration fluctuation eventually becomes only periodic in time.

### 8. Conclusions

In this article we have provided a theoretical confirmation of the efficacy of the isobaric pressure exchanger. The theory predicts the spreading by convective diffusion of salt along each duct inside the pressure exchanger. The effective equation for the slow dispersion along the duct is derived and an explicit formula for the dispersivity (effective diffusivity) is found. The analytical result is used to predict the time scale for the transient mixing to spread across the entire duct length. Moreover, it is shown that even after the transient state is passed, the steady transfer of salt from brine reject to the fresh seawater reentering the membrane is small.

Hence the high efficiency of the isobaric pressure exchanger is theoretically confirmed. Detailed laboratory measurements are not yet available in the literature and would be very worthwhile. For guiding the design it is worth further investigation to predict accurately the magnitude of the pressure transmitted to the feeder pipe. For this purpose the detailed fluid mechanics in the inlet, the outlet and the feeder pipe may have to be taken into account. Other design concerns such as leakage and loud noise would require more elaborate effort in computational modeling.

**Acknowledgements**

CCM acknowledges the support of grants from US-Israel Bi-National Science Foundation and MIT Earth Systems Initiative. YHL is supported by the Postdoctoral Program of the National Taiwan University, the National Research Council of Republic of China, under Contract No. NSC 098-2811-E-002-112 (PI: Chien C. Chang), and in part by MIT. AWKL acknowledges the financial support by Environment and Water Industry Council (EWI) of Singapore, under Project MEWR C651/06/173.

**Appendix**

Fourier expansion of the rectangular pulses with rounded corners

In the positive half period, let

$$W(t) = \begin{cases} 0, & 0 \leq t \leq c; \\ \frac{1}{2} \left[ 1 + \cos \left( \frac{\pi(t-(c+b))}{b} \right) \right], & c \leq t \leq c+b; \\ 1, & c+b \leq t \leq \pi-(c+b); \\ \frac{1}{2} \left[ 1 - \cos \left( \frac{\pi(t-(\pi-c))}{b} \right) \right], & \pi-(c+b) \leq t \leq \pi-c; \\ 0, & \pi-c \leq t \leq \pi \end{cases} \tag{A.1}$$

$$\begin{aligned} \pi W_n &= \int_c^{c+b} \left\{ \frac{1}{2} \left[ 1 + \cos \left( \frac{\pi(t-(c+b))}{b} \right) \right] \right\} \sin(nt) dt \\ &+ \int_{c+b}^{\pi-(c+b)} \sin(nt) dt \\ &+ \int_{\pi-(c+b)}^{\pi-c} \left\{ \frac{1}{2} \left[ 1 - \cos \left( \frac{\pi(t-(\pi-c))}{b} \right) \right] \right\} \sin(nt) dt \\ &= I_1 + I_2 + I_3. \end{aligned} \tag{A.2}$$

We only give the explicit results for  $c = 2b$ ,

$$\begin{aligned} I_1 &= \frac{\cos(nc) - \cos\left(\frac{3nc}{2}\right)}{2n} - \frac{n}{2} \frac{\cos\left(\frac{3nc}{2}\right) + \cos(nc)}{n^2 - \frac{4\pi^2}{c^2}}, \\ I_2 &= \frac{(1 - (-1)^n) \cos\left(\frac{3nc}{2}\right)}{n}, \\ I_3 &= \frac{\cos\left(\frac{3nc}{2}\right) - \cos(nc)}{2n} + \frac{(-1)^n}{2} \cos\left(\frac{2\pi^2}{c}\right) \\ &\times \left\{ \frac{\cos\left(nc + \frac{2\pi^2}{c}\right) + \cos\left(\frac{3nc}{2} + \frac{2\pi^2}{c}\right)}{2\left(n - \frac{2\pi}{c}\right)} \right. \\ &+ \left. \frac{\cos\left(-nc + \frac{2\pi^2}{c}\right) + \cos\left(\frac{-3nc}{2} + \frac{2\pi^2}{c}\right)}{2\left(n + \frac{2\pi}{c}\right)} \right\} \\ &- \frac{(-1)^n}{2} \sin\left(\frac{2\pi^2}{c}\right) \times \left\{ \frac{-\sin\left(nc + \frac{2\pi^2}{c}\right) - \sin\left(\frac{3nc}{2} + \frac{2\pi^2}{c}\right)}{2\left(n - \frac{2\pi}{c}\right)} \right. \\ &- \left. \frac{\sin\left(-nc + \frac{2\pi^2}{c}\right) + \sin\left(\frac{-3nc}{2} + \frac{2\pi^2}{c}\right)}{2\left(n + \frac{2\pi}{c}\right)} \right\}. \end{aligned} \tag{A.3}$$

**Symbols**

- $F'$  — quantity  $F$  in physical dimensions.
- $F$  — normalized quantity  $F$  without dimensions.
- $a_0$  — duct radius.
- $B$  — concentration normalized for unit  $\partial C_0 / \partial x$ .
- $B_m$  —  $m$ -th harmonic amplitude of  $B$ .
- $C$  — brine concentration.
- $C_m$  — concentration perturbation at order  $m$ .
- $\bar{C}$  — time-averaged brine concentration.
- $\langle C \rangle$  — cross-sectional average of duct concentration.
- $\Delta C$  — concentration difference between brine reject and fresh seawater.
- $D$  — molecular diffusivity of brine in water.

$D$	—	dispersion coefficient (Eq. (42)).
$\delta = \sqrt{2\nu/\omega}$	—	dimensional boundary layer thickness.
$\varepsilon$	—	Stokes-Womersley number (Eq. (12)).
$\nu$	—	molecular viscosity.
$L$	—	duct length.
$\omega$	—	rotation frequency.
$r$	—	radial distance from duct center line.
$Re_\delta$	—	Reynolds number (Eq. (1)).
$S_c$	—	Schmidt number.
$t$	—	time.
$T_c$	—	time for concentration interface to diffuse from center to ends of duct.
$u(r, t)$	—	longitudinal flow velocity.
$U$	—	characteristic scale of velocity.
$V(r, t)$	—	velocity correction in the boundary layer.
$V_n$	—	amplitude of the $n$ -th harmonic of $V$ .
$W(t)$	—	flow velocity in the inviscid core.
$W_m$	—	$m$ -th harmonic amplitude of $W$ .
$X$	—	displacement amplitude of concentration interface.
$z_n$	—	boundary layer coordinate for the $n$ -th harmonic (Eq. (17)).

## References

- [1] M. Cakmaker, N. Kayaalp and I. Koyuncu, Desalination of produced water from oil production fields by membrane process, *Desalination*, 222 (2008) 176–186.
- [2] C. Fritzmann, J. Lowenberg, T. Wintgens and T. Melin, State-of-the-art of reverse osmosis desalination, *Desalination*, 216 (2007) 1–76.
- [3] R.L. Stover, Development of a fourth generation energy recovery device, A CTO's Notebook, *Desalination*, 165 (2004) 313–321.
- [4] R.L. Stover, Seawater reverse osmosis with isobaric energy recovery devices, *Desalination*, 203 (2007) 168–175.
- [5] Y-H. Zhou, X-W. Ding, M-W. Mao and Y-Q. Chang, Numerical simulation on a dynamic mixing process in ducts of a rotary pressure exchanger for SWRO, *Desalin. Water Treat.*, 1(2009) 107–113.
- [6] M. Hino, M. Sawamoto and S. Takasu, Experiments on transition to turbulence in an oscillatory pipe flow, *J. Fluid Mech.*, 75 (1976) 193–207.
- [7] M. Ohmi, M. Iguchi, K. Kakehachi and T. Masuda, Transition to turbulence and velocity distribution in an oscillating pipe flow, *Bull. Japan Soc. Mech. Engrs.*, 25 (1982) 365–371.
- [8] K.H. Ahn and M.B. Ibrahim, Laminar/turbulent oscillating flow in circular pipes, *Int. J. Heat Fluid Flow*, 13 (1992) 340–346.
- [9] R. Akhavan, R.D. Kamm and A.H. Shapiro, An investigation of transition to turbulence in bounded oscillatory Stokes flows Part 1. Experiments, *J. Fluid Mech.*, 225 (1991) 395–422.
- [10] R. Akhavan, R.D. Kamm and A.H. Shapiro, An investigation of transition to turbulence in bounded oscillatory Stokes flows Part 2. Numerical simulations, *J. Fluid Mech.*, 225 (1991) 423–444.
- [11] D.M. Ekman and J.B. Grotberg, Experiments on transition to turbulence in oscillatory pipe flow, *J. Fluid Mech.*, 222 (1991) 329–350.
- [12] G.I. Taylor, Dispersion of soluble matter in solvent flowing slowly through a tube, *Proc. R. Soc. London, ser. A.*, 219 (1953) 186–203.
- [13] A. Aris, On the dispersion of a solute in pulsating flow through a tube, *J. Fluid Mech.*, 259 (1960) 370–376.
- [14] P.C. Chatwin, On the longitudinal dispersion of passive contaminant in oscillatory flow in tubes, *J. Fluid Mech.*, 71 (1975) 513–527.
- [15] E.J. Watson, Diffusion in oscillatory pipe flow, *J. Fluid Mech.*, 133 (1983) 233–244.
- [16] J.B. Womersley, Method for the calculation of velocity, rate of flow and viscous drag in the arteries when the pressure gradient is known, *J. Physiol.*, 127 (1955) 553–563.